Journal of Solid Mechanics and Materials Engineering

Vol. 5, No. 2, 2011

Exact Solution of Transient Thermal Stress Problem of a Multilayered Magneto-Electro-Thermoelastic Hollow Cylinder*

Yoshihiro OOTAO** and Masayuki ISHIHARA**

**Department of Mechanical Engineering, Graduate School of Engineering, Osaka Prefecture University, 1-1, Gakuen-cho, Naka-ku, Sakai, Japan

E-mail:ootao@me.osakafu-u.jp

Abstract

This paper presents the theoretical analysis of a multilayered magneto-electro-thermoelastic hollow cylinder under unsteady and uniform surface heating. We obtain the exact solution of the transient thermal stress problem of the multilayered magneto-electro-thermoelastic hollow cylinder in the plane strain state. As an illustration, we perform numerical calculations of a two-layered composite hollow cylinder made of piezoelectric and magnetostrictive materials and investigate the numerical results for temperature change, displacement, stress, and electric and magnetic potential distributions in the transient state. Furthermore, the effects of the coupling, stacking sequence and position of the interface on the stresses, electric potential and magnetic potential are investigated.

Key words: Thermal Stress Problem, Magnetoelectroelastic, Hollow Cylinder, Plane Strain Problem, Transient State

1. Introduction

It has recently been found that composites made of piezoelectric and magnetostrictive materials exhibit the magnetoelectric effect, which is not seen in piezoelectric or magnetostrictive materials [1-3]. These materials are known as multiferroic composites [4]. These composites exhibit a coupling among magnetic, electric, and elastic fields. It is possible to develop a new system of smart composite materials by combining these piezoelectric and magnetostrictive materials with other structural materials.

In the past, various problems in magneto-electro-elastic media that exhibit anisotropic and linear coupling among the magnetic, electric, and elastic fields were analyzed. Examples of static problems are as follows. Pan [5] derived the exact solution of simply supported and multilayered magneto-electro-elastic plates, and Pan and Heyliger [6] derived the exact solution of magneto-electro-elastic laminates in cylindrical bending. Babaei and Chen derived the exact solution of radially polarized and magnetized rotating magneto-electro-elastic hollow and solid cylinders [7]. Ying and Wang derived the exact solution of rotating magneto-electro-elastic composite hollow cylinders [8]. Wang et al. derived an analytical solution of a multilayered magneto-electro-elastic circular plate under simply supported boundary conditions [9]. Examples of dynamic problems are as follows. Wang and Ding analyzed the transient responses of a magneto-electro-elastic hollow sphere [10] and a magneto-electro-elastic composite hollow sphere [11] subjected to spherically symmetric dynamic loads. Anandkumar et al. analyzed the free vibration behavior of

*Received 23 Aug., 2010 (No. 10-0370)
[DOI: 10.1299/jmmp.5.90]

multiphase and layered magneto-electro-elastic beams [12].

Examples of thermal stress problems are as follows. Sunar et al. [13] analyzed thermopiezomagnetic smart structures and Kumarval et al. [14] analyzed a three-layered electro-magneto-elastic strip under steady state conditions using the finite element method. Hou et al. obtained 2D fundamental solutions of a steady point heat source in infinite and semi-infinite orthotropic electro-magneto-thermo-elastic planes [15] and obtained Green's function for a steady point heat source on the surface of a semi-infinite transversely isotropic electro-magneto-thermo-elastic material [16]. Xiong and Ni obtained 2D Green's functions for semi-infinite transversely isotropic electro-magneto-thermo-elastic composites [17]. Gao et al. analyzed the problem of collinear cracks in an electro-magneto-thermo-elastic solid subjected to uniform heat flow at infinity [18]. These studies, however, treated thermal stress problems only under steady temperature distribution. It is well known that thermal stress distributions in a transient state show significant and large response values as compared to those in a steady state. Therefore, transient thermoelastic problems are important. With regard to transient thermal stress problems, Wang and Niraula analyzed transient thermal fracture in transversely isotropic electro-magneto-elastic cylinders [19]. The exact solution of a transient analysis of multilayered magneto-electro-thermoelastic strip subjected to nonuniform heat supply was also obtained [20]. This study [20] discusses the problem in rectangular coordinates. As the multilayered hollow cylinder and hollow sphere have curvature, the behavior of these structures is different from that of the multilayered strip mainly. Though the author et al. studied already a lot of the transient thermal stress problems of the multilayered hollow cylinders [21-23] and multilayered hollow spheres [24], theses studies don't consider a coupling among magnetic, electric, and thermoelastic fields. Furthermore the theoretical analysis of the multilayered hollow cylinder or hollow sphere with a coupling among magnetic, electric, and thermoelastic fields is more difficult than that without the coupling. To the best of the authors' knowledge, the exact analysis of a multilayered magneto-electro-thermoelastic hollow cylinder or hollow sphere under unsteady heat supply has not yet been reported. Here, we present the derivation of an exact solution of the transient thermal stress problem of a multilayered composite hollow cylinder made of magneto-electro-thermoelastic materials under uniform surface heating in a plane strain state. We assumed that the magneto-electro-thermoelastic materials are polarized and magnetized in the radial direction. We carried out numerical calculations for a two-layered hollow cylinder composed of piezoelectric and magnetostrictive materials, and examined the effects of the coupling, stacking sequence and position of the interface on the stresses, electric potential and magnetic potential.

2. Heat conduction problem

We considered a multilayered composite hollow cylinder made of anisotropic and linear magneto-electro-thermoelastic materials. The hollow cylinder's inner and outer radii are denoted by a and b, respectively. r_i is the outer radius of the ith layer. Throughout this article, indices i (=1,2,…, N) are associated with the ith layer from the inner side of a composite hollow cylinder.

We assumed that the multilayered hollow cylinder is initially at zero temperature and its inner and outer surfaces are suddenly heated by surrounding media having constant temperatures T_a and T_b with relative heat transfer coefficients h_a and h_b, respectively. Then, the temperature distribution is one-dimensional, and the transient heat conduction equation for the ith layer is written in the following form:

$$\frac{\partial \overline{T}_i}{\partial \tau} = \overline{\kappa}_{ri}\left(\frac{\partial^2 \overline{T}_i}{\partial \overline{r}^2} + \frac{1}{\overline{r}}\frac{\partial \overline{T}_i}{\partial \overline{r}}\right);\ i = 1,2,\cdots,N \tag{1}$$

The initial and thermal boundary conditions in dimensionless form are

$$\tau = 0; \quad \overline{T}_i = 0 \quad ; \quad i = 1,2,\cdots,N \tag{2}$$

$$\overline{r} = \overline{a}\,; \ \frac{\partial \overline{T}_1}{\partial \overline{r}} - H_a \overline{T}_1 = -H_a \overline{T}_a \tag{3}$$

$$\overline{r} = R_i\,; \ \overline{T}_i = \overline{T}_{i+1} \quad ; \quad i = 1,2,\cdots,N-1 \tag{4}$$

$$\overline{r} = R_i; \overline{\lambda}_{ri} \frac{\partial \overline{T}_i}{\partial \overline{r}} = \overline{\lambda}_{r,i+1} \frac{\partial \overline{T}_{i+1}}{\partial \overline{r}} \ ; \ i = 1,2,\cdots,N-1 \tag{5}$$

$$\overline{r} = 1; \ \frac{\partial \overline{T}_N}{\partial \overline{r}} + H_b \overline{T}_N = H_b \overline{T}_b \tag{6}$$

In Eqs. (1)-(6), we introduced the following dimensionless values:

$$(\overline{T}_i, \overline{T}_a, \overline{T}_b) = (T_i, T_a, T_b)/T_0\,, \ \ (\overline{r}, R_i, \overline{a}) = (r, r_i, a)/b\,, \ \ \tau = \kappa_0 t / b^2\,,$$

$$\overline{\kappa}_{ri} = \kappa_{ri}/\kappa_0\,, \ \ \overline{\lambda}_{ri} = \lambda_{ri}/\lambda_0\,, \ \ (H_a, H_b) = (h_a, h_b)b \tag{7}$$

where T_i is the temperature change; t is time; and T_0, λ_0 and κ_0 are typical values of temperature, thermal conductivity, and thermal diffusivity, respectively. Introducing the Laplace transform with respect to the variable τ, the solution of Eq. (1) can be obtained so as to satisfy the conditions (2)-(6). This solution is written as follows:

$$\overline{T}_i = \frac{1}{F}(\overline{A}_i' + \overline{B}_i' \ln \overline{r}\,) + \sum_{j=1}^{\infty} \frac{2\exp(-\mu_j^2 \tau)}{\mu_j \Delta'(\mu_j)} [\overline{A}_i J_0(\beta_i \mu_j \overline{r}) + \overline{B}_i Y_0(\beta_i \mu_j \overline{r})]\,; i = 1,2,\cdots,N \tag{8}$$

where $J_0(\ )$ and $Y_0(\ )$ are zeroth-order Bessel functions of the first and second kind, respectively. Futhermore, Δ and F are the determinants of $2N \times 2N$ matrices $[a_{kl}]$ and $[e_{kl}]$, respectively; the coefficients $\overline{A}_i$ and $\overline{B}_i$ are defined as determinants of a matrix similar to the coefficient matrix $[a_{kl}]$, in which the (2i-1)th column or 2ith column is replaced with the constant vector $\{c_k\}$, respectively. Similarly, the coefficients $\overline{A}'_i$ and $\overline{B}'_i$ are defined as determinants of a matrix similar to the coefficient matrix $[e_{kl}]$, in which the (2i-1)th column or 2ith column is replaced with the constant vector $\{c_k\}$, respectively. The nonzero elements of the coefficient matrices $[a_{kl}]$ and $[e_{kl}]$ and the constant vector $\{c_k\}$ are given as

$$\begin{aligned}
&a_{1,1} = \beta_1 \mu J_1(\beta_1 \mu \overline{a}) + H_a J_0(\beta_1 \mu \overline{a})\,, \ \ a_{1,2} = \beta_1 \mu Y_1(\beta_1 \mu \overline{a}) + H_a Y_0(\beta_1 \mu \overline{a})\,, \\
&a_{2N,2N-1} = H_b J_0(\beta_N \mu) - \beta_N \mu J_1(\beta_N \mu)\,, \ \ a_{2N,2N-1} = H_b Y_0(\beta_N \mu) - \beta_N \mu Y_1(\beta_N \mu) \\
&a_{2i,2i-1} = J_0(\beta_i \mu R_i)\,, \ \ a_{2i,2i} = Y_0(\beta_i \mu R_i)\,, a_{2i,2i+1} = -J_0(\beta_{i+1} \mu R_i)\,, \\
&a_{2i,2i+2} = -Y_0(\beta_{i+1} \mu R_i)\,, \ \ a_{2i+1,2i-1} = -\overline{\lambda}_{ri} \beta_i \mu J_1(\beta_i \mu R_i)\,, \\
&a_{2i+1,2i} = -\overline{\lambda}_{ri} \beta_i \mu Y_1(\beta_i \mu R_i)\,, \ \ a_{2i+1,2i+1} = \overline{\lambda}_{r,i+1} \beta_{i+1} \mu J_1(\beta_{i+1} \mu R_i)\,, \\
&a_{2i+1,2i+2} = \overline{\lambda}_{r,i+1} \beta_{i+1} \mu Y_1(\beta_{i+1} \mu R_i) \quad ; \ i = 1,2,\cdots,N-1
\end{aligned} \tag{9, 10}$$

$$e_{1,1} = H_a\,, \ \ e_{1,2} = H_a \ln \overline{a} - \frac{1}{\overline{a}}\,, \ \ e_{2N,2N-1} = H_b\,, \ \ e_{2N,2N} = 1 \tag{11}$$

$$\begin{aligned}
&e_{2i,2i-1} = 1\,, \ \ e_{2i,2i} = \ln R_i\,, \ \ e_{2i,2i+1} = -1\,, \ \ e_{2i,2i+2} = -\ln R_i\,, \\
&e_{2i+1,2i} = \frac{\overline{\lambda}_{ri}}{R_i}\,, \ \ e_{2i+1,2i+1} = -\frac{\overline{\lambda}_{r,i+1}}{R_i} \quad ; \quad i = 1,2,\cdots,N-1
\end{aligned} \tag{12}$$

$$c_1 = H_a \overline{T}_a\,, \ \ c_{2N} = H_b \overline{T}_b \tag{13}$$

In Eq. (8), $\Delta'(\mu_j)$ and β_i are

$$\Delta'(\mu_j) = \left.\frac{d\Delta}{d\mu}\right|_{\mu=\mu_j}\,, \qquad \beta_i = \frac{1}{\sqrt{\overline{\kappa}_{ri}}} \tag{14}$$

and μ_j is the jth positive root of the following transcendental equation

$$\Delta(\mu) = 0 \tag{15}$$

3. Thermal stress problem

We developed the analysis of a multilayered magneto-electro-thermoelastic hollow cylinder as a plane strain problem. The displacement-strain relations are expressed in dimensionless form as follows:

$$\bar{\varepsilon}_{rri} = \bar{u}_{ri,\bar{r}}, \quad \bar{\varepsilon}_{\theta\theta i} = \bar{u}_{ri}/\bar{r}, \quad \bar{\varepsilon}_{zzi} = \bar{\gamma}_{r\theta i} = \bar{\gamma}_{rzi} = \bar{\gamma}_{\theta zi} = 0 \tag{16}$$

where the comma denotes partial differentiation with respect to the variable that follows. For the anisotropic and linear magneto-electro-thermoelastic material, the constitutive relations are expressed in dimensionless form as follows:

$$\begin{aligned}
\bar{\sigma}_{rri} &= \bar{C}_{11i}\bar{\varepsilon}_{rri} + \bar{C}_{12i}\bar{\varepsilon}_{\theta\theta i} - \bar{\beta}_{ri}\bar{T}_i - \bar{e}_{1i}\bar{E}_{ri} - \bar{q}_{1i}\bar{H}_{ri}, \\
\bar{\sigma}_{\theta\theta i} &= \bar{C}_{12i}\bar{\varepsilon}_{rri} + \bar{C}_{22i}\bar{\varepsilon}_{\theta\theta i} - \bar{\beta}_{\theta i}\bar{T}_i - \bar{e}_{2i}\bar{E}_{ri} - \bar{q}_{2i}\bar{H}_{ri}, \\
\bar{\sigma}_{zzi} &= \bar{C}_{13i}\bar{\varepsilon}_{rri} + \bar{C}_{23i}\bar{\varepsilon}_{\theta\theta i} - \bar{\beta}_{zi}\bar{T}_i - \bar{e}_{3i}\bar{E}_{ri} - \bar{q}_{3i}\bar{H}_{ri}
\end{aligned} \tag{17}$$

where

$$\begin{aligned}
\bar{\beta}_{ri} &= \bar{C}_{11i}\bar{\alpha}_{ri} + \bar{C}_{12i}\bar{\alpha}_{\theta i} + \bar{C}_{13i}\bar{\alpha}_{zi}, \\
\bar{\beta}_{\theta i} &= \bar{C}_{12i}\bar{\alpha}_{ri} + \bar{C}_{22i}\bar{\alpha}_{\theta i} + \bar{C}_{23i}\bar{\alpha}_{zi}, \\
\bar{\beta}_{zi} &= \bar{C}_{13i}\bar{\alpha}_{ri} + \bar{C}_{23i}\bar{\alpha}_{\theta i} + \bar{C}_{33i}\bar{\alpha}_{zi}
\end{aligned} \tag{18}$$

The constitutive equations for the electric and the magnetic fields in dimensionless form are given as

$$\bar{D}_{ri} = \bar{e}_{1i}\bar{\varepsilon}_{rri} + \bar{e}_{2i}\bar{\varepsilon}_{\theta\theta i} + \bar{\eta}_{1i}\bar{E}_{ri} + \bar{d}_{1i}\bar{H}_{ri} + \bar{p}_{1i}\bar{T}_i \tag{19}$$

$$\bar{B}_{ri} = \bar{q}_{1i}\bar{\varepsilon}_{rri} + \bar{q}_{2i}\bar{\varepsilon}_{\theta\theta i} + \bar{d}_{1i}\bar{E}_{ri} + \bar{\mu}_{1i}\bar{H}_{ri} + \bar{m}_{1i}\bar{T}_i \tag{20}$$

The relation between the electric field intensity and the electric potential ϕ_i in dimensionless form is defined as

$$\bar{E}_{ri} = -\bar{\phi}_{i,\bar{r}} \tag{21}$$

The relation between the magnetic field intensity and the magnetic potential ψ_i in dimensionless form is defined as

$$\bar{H}_{ri} = -\bar{\psi}_{i,\bar{r}} \tag{22}$$

The equilibrium equation is expressed in dimensionless form as follows:

$$\bar{\sigma}_{rri,\bar{r}} + (\bar{\sigma}_{rri} - \bar{\sigma}_{\theta\theta i})/\bar{r} = 0 \tag{23}$$

If the electric charge density is absent, the equations of electrostatics and magnetostatics are expressed in dimensionless form as follows:

$$\bar{D}_{ri,\bar{r}} + \bar{D}_{ri}/\bar{r} = 0 \tag{24}$$

$$\bar{B}_{ri,\bar{r}} + \bar{B}_{ri}/\bar{r} = 0 \tag{25}$$

In Eqs. (16)-(25), the following dimensionless values are introduced:

$$\bar{\sigma}_{kli} = \frac{\sigma_{kli}}{\alpha_0 Y_0 T_0}, \quad (\bar{\varepsilon}_{kli}, \bar{\gamma}_{kli}) = \frac{(\varepsilon_{kli}, \gamma_{kli})}{\alpha_0 T_0}, \quad \bar{u}_{ri} = \frac{u_{ri}}{\alpha_0 T_0 b}, \quad \bar{\alpha}_{ki} = \frac{\alpha_{ki}}{\alpha_0}, \quad \bar{C}_{kli} = \frac{C_{kli}}{Y_0},$$

$$\overline{D}_{ri}=\frac{D_{ri}}{\alpha_0 Y_0 T_0 |d_0|},\quad \overline{B}_{ri}=\frac{B_{ri}|d_0|\kappa_0}{b\alpha_0 T_0},\quad \overline{\phi}_i=\frac{\phi_i|d_0|}{\alpha_0 T_0 b},\quad \overline{\psi}_i=\frac{\psi_i}{|d_0|\kappa_0\alpha_0 Y_0 T_0},$$

$$\overline{e}_{ki}=\frac{e_{ki}}{Y_0|d_0|},\quad \overline{\eta}_{1i}=\frac{\eta_{1i}}{Y_0|d_0|^2},\quad \overline{q}_{ki}=\frac{q_{ki}\kappa_0|d_0|}{b},\quad \overline{\mu}_{1i}=\frac{\mu_{1i}\kappa_0^2|d_0|^2 Y_0}{b^2},$$

$$\overline{d}_{1i}=\frac{\kappa_0 d_{1i}}{b},\quad \overline{p}_{1i}=\frac{p_{1i}}{\alpha_0 Y_0|d_0|},\quad \overline{m}_{1i}=\frac{m_{1i}\kappa_0|d_0|}{b\alpha_0},\quad \overline{E}_{ri}=\frac{E_{ri}|d_0|}{\alpha_0 T_0},$$

$$\overline{H}_{ri}=\frac{H_{ri}b}{|d_0|\kappa_0\alpha_0 Y_0 T_0} \tag{26}$$

where σ_{kli} are the stress components; (ε_{kli}, γ_{kli}) are the strain components; u_{ri} is the displacement in the r direction; α_{ki} are the coefficients of linear thermal expansion; C_{kli} are the elastic stiffness constants; D_{ri} is the electric displacement in the r direction; B_{ri} is the magnetic flux density in the r direction; e_{ki} are the piezoelectric coefficients; η_{1i} is the dielectric constant; p_{1i} is the pyroelectric constant; q_{ki} are the piezomagnetic coefficients; μ_{1i} is the magnetic permeability coefficient; d_{1i} is the magnetoelectric coefficient; m_{1i} is the pyromagnetic constant; and α_0, Y_0 and d_0 are typical values of the coefficient of linear thermal expansion, Young's modulus, and piezoelectric modulus, respectively.

Substituting Eqs. (16), (21), and (22) into Eqs. (17), (19), and (20) and later into Eqs. (23)-(25), the governing equations of the displacement u_{ri}, electric potential ϕ_i, and magnetic potential ψ_i in the dimensionless form are written as

$$\begin{aligned}&\overline{C}_{11i}\overline{u}_{ri,\overline{r}\overline{r}}+\overline{C}_{11i}\overline{u}_{ri,\overline{r}}\,\overline{r}^{-1}-\overline{C}_{22i}\overline{u}_{ri}\overline{r}^{-2}+\overline{e}_{1i}\overline{\phi}_{i,\overline{r}\overline{r}}+(\overline{e}_{1i}-\overline{e}_{2i})\overline{\phi}_{i,\overline{r}}\,\overline{r}^{-1}\\&\quad+\overline{q}_{1i}\overline{\psi}_{i,\overline{r}\overline{r}}+(\overline{q}_{1i}-\overline{q}_{2i})\overline{\psi}_{i,\overline{r}}\,\overline{r}^{-1}=(\overline{\beta}_{ri}-\overline{\beta}_{\theta i})\overline{T}_i\overline{r}^{-1}+\overline{\beta}_{ri}\overline{T}_{i,\overline{r}}\end{aligned} \tag{27}$$

$$\begin{aligned}&\overline{e}_{1i}\overline{u}_{ri,\overline{r}\overline{r}}+(\overline{e}_{1i}+\overline{e}_{2i})\overline{u}_{ri,\overline{r}}\,\overline{r}^{-1}-\overline{\eta}_{1i}\overline{\phi}_{i,\overline{r}\overline{r}}-\overline{\eta}_{1i}\overline{\phi}_{i,\overline{r}}\,\overline{r}^{-1}-\overline{d}_{1i}\overline{\psi}_{i,\overline{r}\overline{r}}-\overline{d}_{1i}\overline{\psi}_{i,\overline{r}}\,\overline{r}^{-1}\\&\quad=-\overline{p}_{1i}(\overline{T}_{i,\overline{r}}+\overline{T}_i\overline{r}^{-1})\end{aligned} \tag{28}$$

$$\begin{aligned}&\overline{q}_{1i}\overline{u}_{ri,\overline{r}\overline{r}}+(\overline{q}_{1i}+\overline{q}_{2i})\overline{u}_{ri,\overline{r}}\,\overline{r}^{-1}-\overline{d}_{1i}\overline{\phi}_{i,\overline{r}\overline{r}}-\overline{d}_{1i}\overline{\phi}_{i,\overline{r}}\,\overline{r}^{-1}-\overline{\mu}_{1i}\overline{\psi}_{i,\overline{r}\overline{r}}-\overline{\mu}_{1i}\overline{\psi}_{i,\overline{r}}\,\overline{r}^{-1}\\&\quad=-\overline{m}_{1i}(\overline{T}_{i,\overline{r}}+\overline{T}_i\overline{r}^{-1})\end{aligned} \tag{29}$$

If the inner and outer surfaces of the multilayered magneto-electro-thermoelastic hollow cylinder are traction free, and the interfaces of each adjoining layer are perfectly bonded, then the boundary conditions of inner and outer surfaces and the conditions of continuity at the interfaces can be represented as follows:

$$\begin{aligned}&\overline{r}=\overline{a};\quad \overline{\sigma}_{rr1}=0,\\&\overline{r}=R_i;\quad \overline{\sigma}_{rri}=\overline{\sigma}_{rr,i+1},\overline{u}_{ri}=\overline{u}_{r,i+1}\quad ;i=1,\cdots,N-1,\\&\overline{r}=1;\quad \overline{\sigma}_{rrN}=0\end{aligned} \tag{30}$$

The boundary conditions in the radial direction for the electric and magnetic fields are expressed as

$$\overline{r}=\overline{a};\quad \overline{D}_{r1}=0,\overline{B}_{r1}=0\ \text{ or }\ \overline{\phi}_1=0,\overline{\psi}_1=0,$$

$$\overline{r}=R_i;\quad \overline{D}_{ri}=\overline{D}_{r,i+1},\overline{B}_{ri}=\overline{B}_{r,i+1},\overline{\phi}_i=\overline{\phi}_{i+1},\ \overline{\psi}_i=\overline{\psi}_{i+1}\quad ;i=1,\cdots,N-1,$$

$$\bar{r}=1;\quad \overline{D}_{rN}=0,\ \overline{B}_{rN}=0\quad \text{or}\quad \bar{\phi}_N=0,\bar{\psi}_N=0 \tag{31}$$

The solutions of Eqs. (27)-(29) are assumed in the following form:

$$\bar{u}_{ri}=\bar{u}_{rci}+\bar{u}_{rpi},\ \ \bar{\phi}_i=\bar{\phi}_{ci}+\bar{\phi}_{pi},\ \ \bar{\psi}_i=\bar{\psi}_{ci}+\bar{\psi}_{pi} \tag{32}$$

In Eq. (32), the first term on the right-hand side gives the homogeneous solution and the second term gives the particular solution. The homogeneous solutions of Eq. (32) can be expressed as follows:

$$\bar{u}_{rci}=C_{1i}\bar{r}^{-1}+C_{3i}\bar{r}^{m_i}+C_{4i}\bar{r}^{-m_i},$$

$$\bar{\phi}_{ci}=\frac{\overline{C}_{11i}}{\bar{e}_{1i}}(C_{8i}+C_{7i}\ln\bar{r}+g_{5i}C_{3i}\bar{r}^{m_i}+g_{6i}C_{4i}\bar{r}^{-m_i}),$$

$$\bar{\psi}_{ci}=\frac{\overline{C}_{11i}}{\bar{q}_{1i}}(C_{6i}+C_{5i}\ln\bar{r}+g_{2i}C_{3i}\bar{r}^{m_i}+g_{3i}C_{4i}\bar{r}^{-m_i}) \tag{33}$$

where

$$m_i=\sqrt{-\frac{b_{2i}}{b_{4i}}},\ \ b_{2i}=-[\alpha_i\gamma_i+\beta_{ei}^2+\frac{(\beta_{qi}\gamma_i-\beta_{ei}\beta_{di})^2}{\delta_i\gamma_i-\beta_{di}^2}],$$

$$b_{4i}=1+\gamma_i+\frac{(\gamma_i-\beta_{di})^2}{\delta_i\gamma_i-\beta_{di}^2},\ \ \alpha_i=\frac{\overline{C}_{22i}}{\overline{C}_{11i}},\ \ \beta_{ei}=\frac{\bar{e}_{2i}}{\bar{e}_{1i}},\ \ \beta_{qi}=\frac{\bar{q}_{2i}}{\bar{q}_{1i}},$$

$$\beta_{di}=\frac{\overline{C}_{11i}\bar{d}_{1i}}{\bar{e}_{1i}\bar{q}_{1i}},\ \ \bar{\gamma}_i=\frac{\overline{C}_{11i}\bar{\eta}_{1i}}{\bar{e}_{1i}^2},\ \ \delta_i=\frac{\overline{C}_{11i}\bar{\mu}_{1i}}{\bar{q}_{1i}^2},$$

$$g_{2i}=\frac{1}{m_i(\delta_i\gamma_i-\beta_{di}^2)}[m_i(\gamma_i-\beta_{di})+\beta_{qi}\gamma_i-\beta_{ei}\beta_{di}],$$

$$g_{3i}=\frac{1}{m_i(\delta_i\gamma_i-\beta_{di}^2)}[m_i(\gamma_i-\beta_{di})-\beta_{qi}\gamma_i+\beta_{ei}\beta_{di}],$$

$$g_{5i}=\frac{1}{m_i\gamma_i}[m_i(1-g_{2i}\beta_{di})+\beta_{ei}],\ \ g_{6i}=\frac{1}{m_i\gamma_i}[m_i(1-g_{3i}\beta_{di})-\beta_{ei}] \tag{34}$$

In Eq. (33), C_{ki} ($k=1,3\cdots,8$) are unknown constants. We have the following relation.

$$\alpha_iC_{1i}+\beta_{ei}C_{7i}+\beta_{qi}C_{5i}=0 \tag{35}$$

The details of the derivation of the Eqs. (33) and (34) are omitted here.

It is difficult to obtain the particular solutions using the temperature solution of Eq. (8). In order to obtain the particular solutions, series expansions of Bessel functions given in Eq. (8) are used. Eq. (8) can be written in the following way:

$$\overline{T}_i(\bar{r}_i,\tau)=\sum_{n=0}^{\infty}[a_{in}(\tau)\bar{r}^{2n}+b_{in}(\tau)\bar{r}^{2n}\ln\bar{r}] \tag{36}$$

where

$$a_{in}(\tau)=\frac{\overline{A}_i'}{F}\delta_{0n}$$
$$+\sum_{j=1}^{\infty}\frac{2\exp(-\mu_j^2\tau)}{\mu_j\Delta'(\mu_j)}[\overline{A}_i+\frac{2}{\pi}\overline{B}_i(\gamma^*+\ln\frac{\beta_i\mu_j}{2}-\sum_{m=1}^{n}\frac{1}{m})]\frac{(-1)^n}{n!n!}\left(\frac{\beta_i\mu_j}{2}\right)^{2n},$$

$$b_{in}(\tau)=\frac{\bar{B}_i'}{F}\delta_{0n}+\sum_{j=1}^{\infty}\frac{2\exp(-\mu_j^2\tau)}{\mu_j\Delta'(\mu_j)}\frac{2}{\pi}\bar{B}_i\frac{(-1)^n}{n!n!}\left(\frac{\beta_i\mu_j}{2}\right)^{2n} \tag{37}$$

Here, δ_{0n} is the Kronecker delta. The particular solutions $\bar{u}_{rpi}$, $\bar{\phi}_{pi}$, and $\bar{\psi}_{pi}$ are obtained in the following forms:

$$\bar{u}_{rpi}=\sum_{n=0}^{\infty}[f_{ani}(\tau)\bar{r}^{2n+1}+f_{bni}(\tau)\bar{r}^{2n+1}\ln\bar{r}],$$

$$\bar{\phi}_{pi}=\sum_{n=0}^{\infty}[h_{ani}(\tau)\bar{r}^{2n+1}+h_{bni}(\tau)\bar{r}^{2n+1}\ln\bar{r}],$$

$$\bar{\psi}_{pi}=\sum_{n=0}^{\infty}[g_{ani}(\tau)\bar{r}^{2n+1}+g_{bni}(\tau)\bar{r}^{2n+1}\ln\bar{r}] \tag{38}$$

Expressions for $f_{ani}(\tau)$, $f_{bni}(\tau)$, $h_{ani}(\tau)$, $h_{bni}(\tau)$, $g_{ani}(\tau)$ and $g_{bni}(\tau)$, in Eq. (38) have been omitted here for brevity. Then, the stress components, electric displacement, and magnetic flux density can be evaluated from Eq. (33). Details of the solutions are omitted from here for brevity. The unknown constants in the homogeneous solutions are determined so as to satisfy the boundary conditions in (30) and (31).

4. Numerical results

In order to illustrate the foregoing analysis, we consider a two-layered hollow cylinder composed of piezoelectric and magnetostrictive layers. The two-layered structure is a fundamental model of the multilayered structures, and suites to investigate the effect of stacking sequence of the piezoelectric and magnetostrictive layers. The piezoelectric layer is made up of $BaTiO_3$, and the magnetostrictive layer is made up of $CoFe_2O_4$. Two kinds of two-layered hollow cylinders are investigated. Case 1 shows the stacking sequence $BaTiO_3/CoFe_2O_4$ and case 2 shows the stacking sequence $CoFe_2O_4/BaTiO_3$. We assume that the outer surface of the two-layered hollow cylinder is heated. Then, numerically calculable parameters of the heat condition and shape are presented as follows:

$$H_a=H_b=1.0,\ \bar{T}_a=0,\ \ \bar{T}_b=1,\ N=2,$$

$$\bar{a}=0.7,\ R_1=0.75,0.8,0.85,0.9,0.95,\ b=0.01m \tag{39}$$

The following are material constants considered for $BaTiO_3$:

$$\alpha_\theta=\alpha_z=15.7\times10^{-6}\,1/K,\ \alpha_r=6.4\times10^{-6}\,1/K,$$

$$C_{22}=C_{33}=166\,GPa,\ C_{23}=77\,GPa,\ C_{12}=C_{13}=78\,GPa,\ C_{11}=162\,GPa$$

$$e_2=e_3=-4.4\,C/m^2,\ e_1=18.6\,C/m^2,\ \eta_1=12.6\times10^{-9}\,C^2/Nm^2,$$

$$p_1=2\times10^{-4}\,C^2/m^2K,\ \mu_1=10\times10^{-6}\,Ns^2/C^2,\ \lambda_r=2.5\,W/mK,$$

$$\kappa_r=0.88\times10^{-6}\ m^2/s \tag{40}$$

The corresponding constants for $CoFe_2O_4$ are

$$\alpha_r=\alpha_\theta=\alpha_z=10\times10^{-6}\,1/K,\ C_{22}=C_{33}=286\,GPa$$

$$C_{23}=173\,GPa,\ C_{12}=C_{13}=170.5\,GPa,\ C_{11}=269.5\,GPa,$$

$$q_2=q_3=580.3\,N/Am,\ q_1=699.7\,N/Am,\ \eta_1=0.093\times10^{-9}\,C^2/Nm^2,$$

$$\mu_1 = 157\times10^{-6}\ Ns^2/C^2,\quad \lambda_r = 3.2\ W/mK,$$

$$\kappa_r = 0.77\times10^{-6}\ m^2/s \tag{41}$$

The typical values of material parameters such as κ_0, λ_0, α_0, Y_0, and d_0, used to normalize the numerical data, based on those of $BaTiO_3$ are as follows:

$$\kappa_0 = \kappa_r,\quad \lambda_0 = \lambda_r,\quad \alpha_0 = \alpha_\theta,\quad Y_0 = 116\,GPa,\quad d_0 = -78\times10^{-12}\,C/N \tag{42}$$

In the numerical calculations, the boundary conditions at the surfaces for the electric and magnetic fields are expressed as

$$\bar{r} = \bar{a};\quad \overline{D}_{r1} = 0, \overline{B}_{r1} = 0,$$

$$\bar{r} = 1;\quad \bar{\phi}_N = 0, \overline{\psi}_N = 0 \tag{43}$$

The numerical results for case 1 and $R_1 = 0.85$ are shown in Figures 1-7. Figure 1 shows the variation of temperature change along the radial direction. Figure 2 shows the variation of displacement $\bar{u}_r$ along the radial direction. From Figures 1 and 2, it is clear that the temperature and displacement increase with time and have the largest values in steady state. Figures 3-5 show variations of thermal stresses $\bar{\sigma}_{rr}$, $\bar{\sigma}_{\theta\theta}$, and $\bar{\sigma}_{zz}$, respectively, along the radial direction. Figure 3 reveals that the maximum tensile stress of $\bar{\sigma}_{rr}$ occurs in the transient state and the maximum compressive stress of $\bar{\sigma}_{rr}$ occurs in the steady state. From Figure 4, it is clear that the compressive stress occurs in the first layer and tensile stress occurs in the second layer. From Figure 5, it is clear that the compressive stress occurs inside the hollow cylinder and its absolute value increases with time. Figures 6

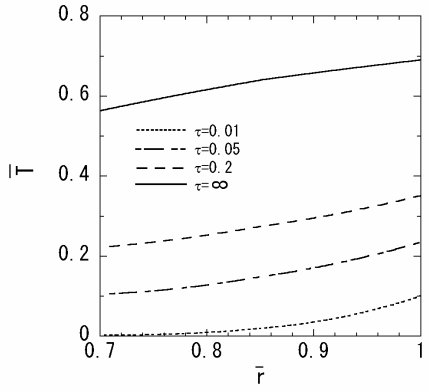

Fig.1 Temperature change (Case 1)

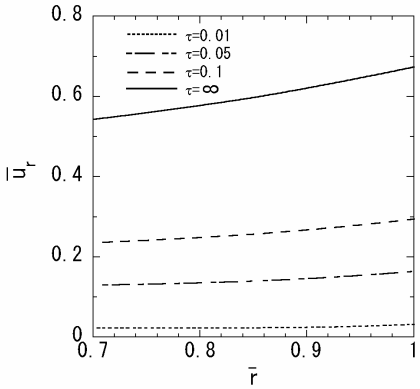

Fig.2 Displacement $\bar{u}_r$ (Case 1)

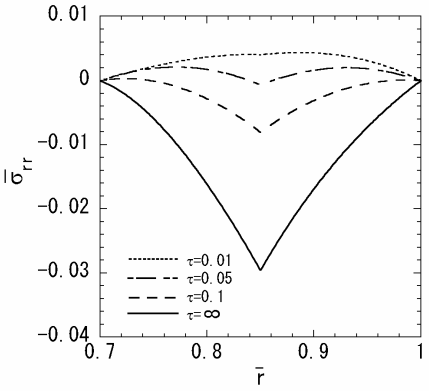

Fig.3 Thermal stress $\bar{\sigma}_{rr}$ (Case 1)

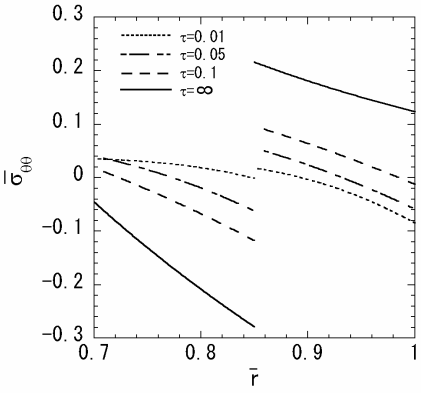

Fig.4 Thermal stress $\bar{\sigma}_{\theta\theta}$ (Case 1)

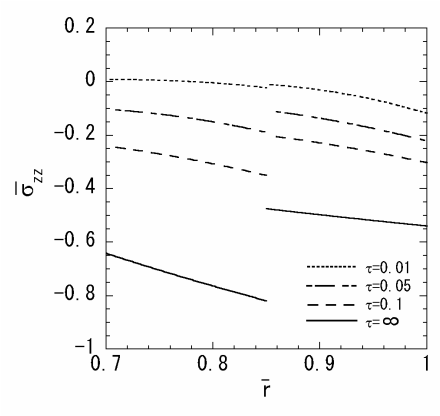

Fig.5 Thermal stress $\bar{\sigma}_{zz}$ (Case 1)

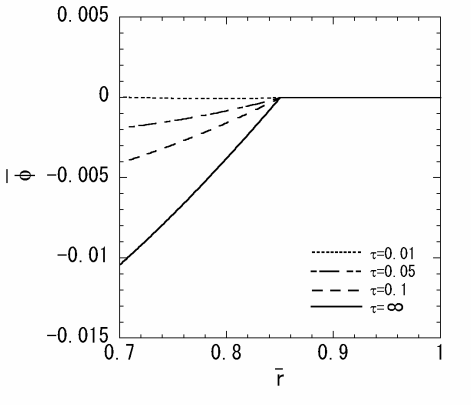

Fig.6 Electric potential $\bar{\phi}$ (Case 1)

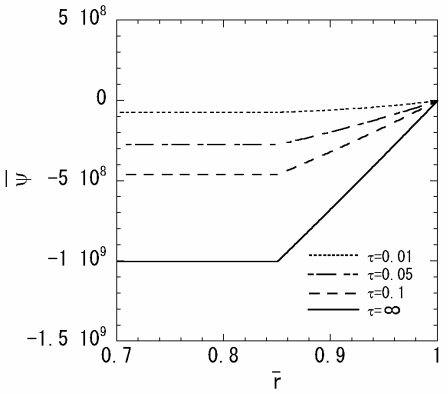

Fig.7 Magnetic potential $\bar{\psi}$ (Case 1)

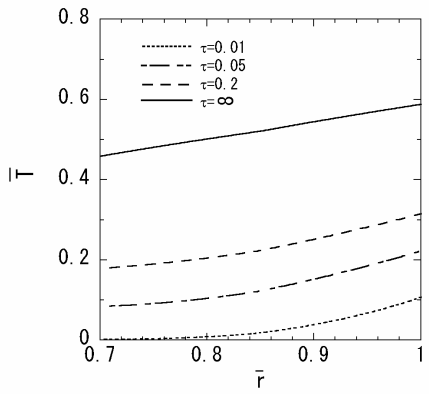

Fig.8 Temperature change (Case 2)

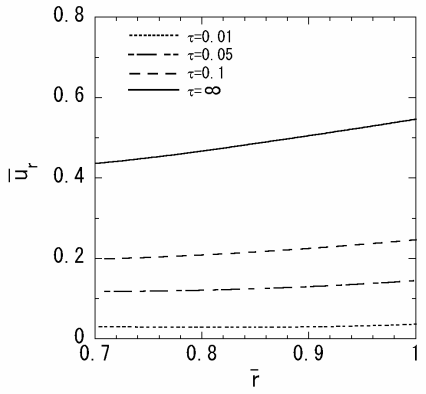

Fig.9 Displacement $\bar{u}_r$ (Case 2)

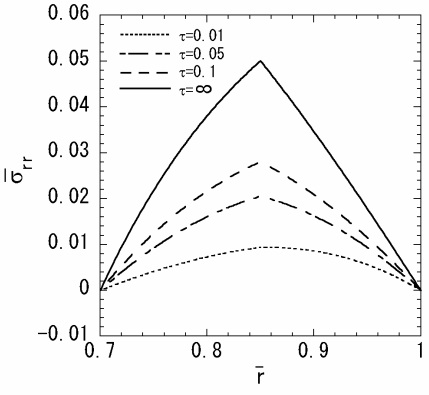

Fig.10 Thermal stress $\bar{\sigma}_{rr}$ (Case 2)

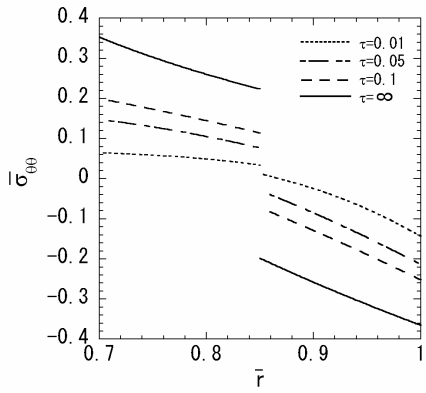

Fig.11 Thermal stress $\bar{\sigma}_{\theta\theta}$ (Case 2)

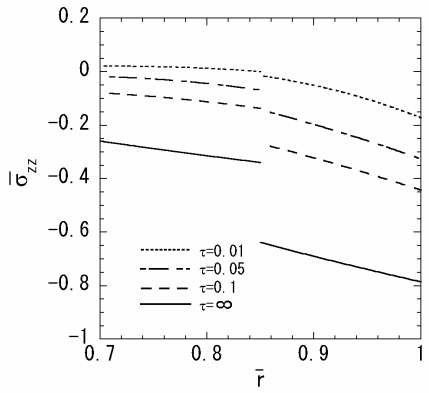

Fig.12 Thermal stress $\bar{\sigma}_{zz}$ (Case 2)

and 7 show the variations of electric potential $\bar{\phi}$ and magnetic potential $\bar{\psi}$, respectively, along the radial direction. Figure 6 reveals that the absolute value of the electric potential increases with time, except during the early stage of heating, and attains its maximum value in the steady state. The electric potential is almost zero in the second layer, i.e. the magnetostrictive layer. From Figure 7, it is clear that the absolute value of the magnetic potential increases with time and attains its maximum value in the steady state. The magnetic potential is almost constant in the first layer, i.e. the piezoelectric layer.

The numerical results for case 2 and $R_1 = 0.85$ are shown in Figures 8-14. Figure 8 shows the variation of temperature change along the radial direction. Figure 9 shows the variation of displacement $\bar{u}_r$ along the radial direction. From Figures 1, 2, 8, and 9, it is

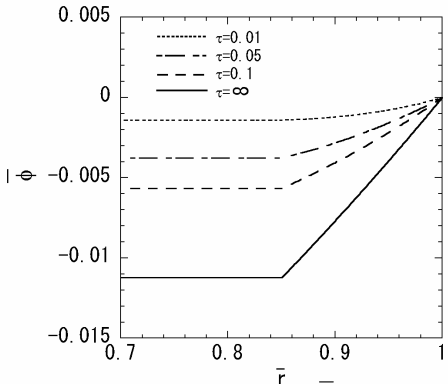

Fig.13 Electric potential $\bar{\phi}$ (Case 2)

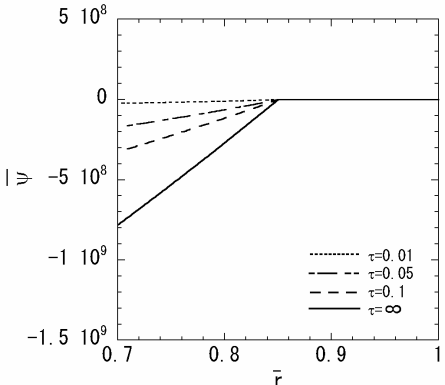

Fig.14 Magnetic potential $\bar{\psi}$ (Case 2)

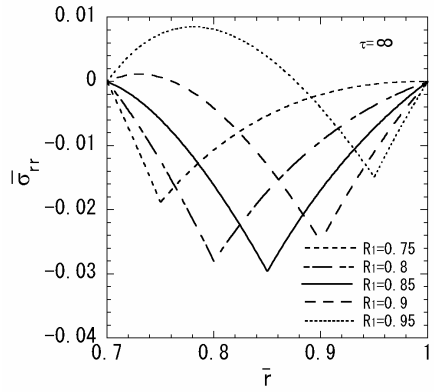

Fig.15 Thermal stress $\bar{\sigma}_{rr}$ (Case 1, $\tau = \infty$)

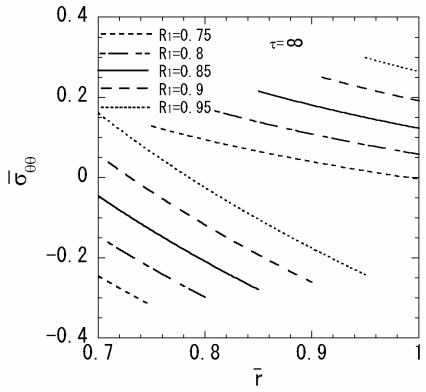

Fig.16 Thermal stress $\bar{\sigma}_{\theta\theta}$ (Case 1, $\tau = \infty$)

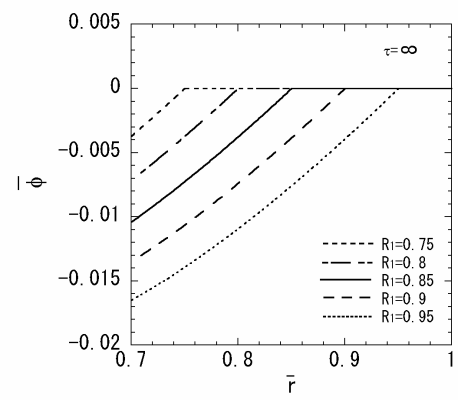

Fig.17 Electric potential $\bar{\phi}$ (Case 1, $\tau = \infty$)

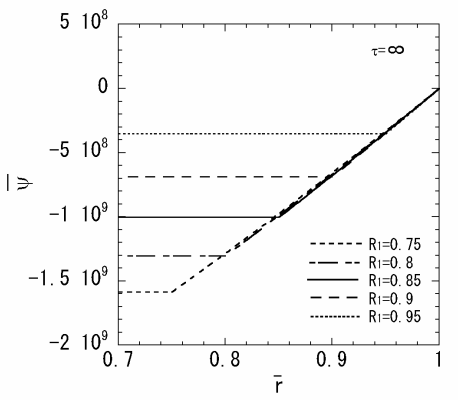

Fig.18 Magnetic potential $\bar{\psi}$ (Case 1, $\tau = \infty$)

clear that the temperature increase and displacement $\bar{u}_r$ of case 1 are larger than those of case 2. Figures 10-12 show the variations of thermal stresses $\bar{\sigma}_{rr}$, $\bar{\sigma}_{\theta\theta}$, and $\bar{\sigma}_{zz}$, respectively, along the radial direction. From Figure 10, it is clear that the maximum tensile stress occurs in the steady state. Figure 11 reveals that tensile stress occurs in the first layerand compressive stress occurs in the second layer. Figure 12 reveals that compressive stress occurs inside the hollow cylinder and its absolute value increases with time. The maximum compressive stress occurs in the second layer. Figures 13 and 14 show the variations of electric potential $\bar{\phi}$ and magnetic potential $\bar{\psi}$, respectively, along the radial direction. From these figures, it is clear that the absolute values of the electric and magnetic potential increases with time, and attain their maximum value in the steady state. The electric potential is almost constant in the first layer, i.e. the magnetostrictive layer. In contrast, the magnetic potential is almost zero in the second layer, i.e. the piezoelectric layer.

In order to assess the influence of the position of the interface between both the layers, numerical results for case 1 and $R_1 = 0.75, 0.8, 0.85, 0.9, 0.95$ were obtained; these results are shown in Figures 15-18. Figures 15 and 16 show the variations of thermal stresses $\bar{\sigma}_{rr}$ and $\bar{\sigma}_{\theta\theta}$, respectively, in the steady state. Figures 17 and 18 show the variations of electric and magnetic potential, respectively, in the steady state. From Figures 15 and 16, it is clear that the distribution of the thermal stress $\bar{\sigma}_{rr}$ changes substantially with a change in the parameter R_1, whereas the maximum tensile stress $\bar{\sigma}_{\theta\theta}$ increases with an increase R_1. It can be seen from Figures 17 and 18 that the absolute values of electric potential increase and those of magnetic potential decrease with an increase in R_1.

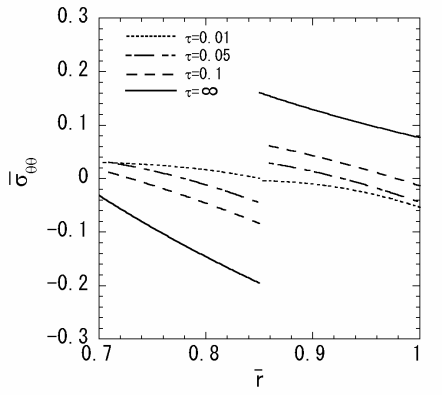

Fig.19 Thermal stress $\bar{\sigma}_{\theta\theta}$
($BaTiO_3/CoFe_2O_4$, Thermoelastic)

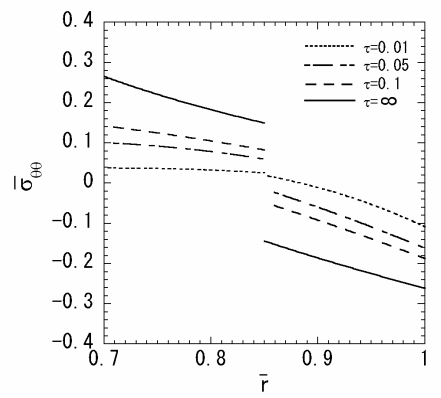

Fig.20 Thermal stress $\bar{\sigma}_{\theta\theta}$
($CoFe_2O_4/BaTiO_3$, Thermoelastic)

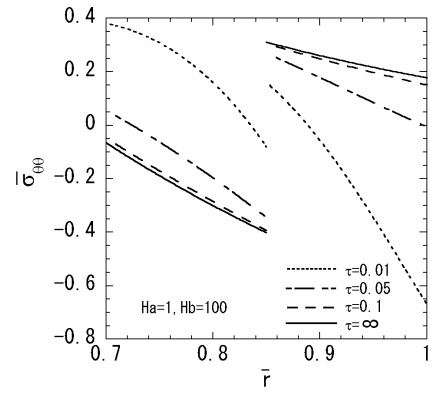

Fig.21 Thermal stress $\bar{\sigma}_{\theta\theta}$
($BaTiO_3/CoFe_2O_4$, $H_a=1, H_b=100$)

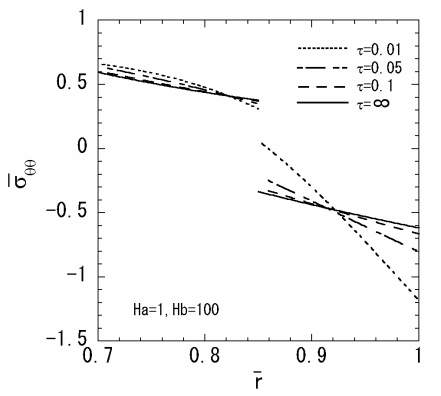

Fig.22 Thermal stress $\bar{\sigma}_{\theta\theta}$
($CoFe_2O_4/BaTiO_3$, $H_a=1, H_b=100$)

In order to assess the influence of coupling effect among magnetic, electric, and thermoelastic fields on the stress, Figures 19 and 20 show the numerical results for the two-layered thermoelastic hollow cylinder without the piezoelectric, piezomagnetic and magnetoelectric effects. The variations of thermal stress $\bar{\sigma}_{\theta\theta}$ along the radial direction for the stacking sequence $BaTiO_3/CoFe_2O_4$ and $CoFe_2O_4/BaTiO_3$ are shown in Figures 19 and 20, respectively. From Figures 4, 11, 19 and 20, it can be seen that the thermal stress considered the coupling effect shows larger than that without the coupling effect.

As the second numerical example, we consider the numerical parameters of heat conduction and shape as follows:

$$H_a = 1.0,\ H_b = 100.0,\ \bar{T}_a = 0,\ \bar{T}_b = 1,\ N = 2,\ \bar{a} = 0.7,\ R_1 = 0.85 \quad (44)$$

Figures 21 and 22 show the variations of thermal stress $\bar{\sigma}_{\theta\theta}$ along the radial direction for the stacking sequence $BaTiO_3/CoFe_2O_4$ and $CoFe_2O_4/BaTiO_3$, respectively. From Figures 21 and 22, it is clear that the maximum tensile stress occurs in the first layer in the transient state without distinction of the stacking sequence. The transient thermal stress analysis is important from above viewpoint.

The previous paper [20] shows the numerical results of two-dimensional problem for simply supported multilayered strip due to local surface heating, and investigates the behaviors which contain the influence by the local heating under the condition without the bending restriction. The behavior of the displacements in the x and y directions, the stresses $\bar{\sigma}_{xx}$, $\bar{\sigma}_{yy}$, $\bar{\sigma}_{zz}$, and $\bar{\sigma}_{zx}$, the electric and magnetic potential is two-dimensional. On the other hand, as this problem is a one-dimensional problem, the numerical results show the behaviors of the displacement, the normal stresses $\bar{\sigma}_{rr}$, $\bar{\sigma}_{\theta\theta}$, $\bar{\sigma}_{zz}$, and the electric and magnetic potential in the radial direction. The mageno-electro-thermoelastic response of the multilayered strip and that of the multilayered hollow cylinder are different. As the multilayered hollow cylinder has curvature and is under restriction to the circumstance direction, especially, the behavior of the in-plane stress $\bar{\sigma}_{\theta\theta}$ is different from that of the in-plane stress $\bar{\sigma}_{xx}$ in the multilayered strip mainly.

5. Conclusion

In this study, we obtained the exact solution of the transient thermal stress problem of a multilayered magneto-electro-thermoelastic hollow cylinder under uniform surface heating as a plane strain problem by solving the governing equations of the displacement, electric potential, and magnetic potential. In order to obtain the particular solutions, series expansions of Bessel functions in temperature solution were used. We can evaluate that the electric and magnetic fields of the hollow cylinder in a transient state due to the analysis with a coupling among magnetic, electric, and thermoelastic fields. As an illustration, we carried out numerical calculations for a two-layered hollow cylinder composed of piezoelectric and magnetostrictive materials, and examined its behavior in the transient state in terms of temperature change, displacement, stress, and electric and magnetic potential distributions. Furthermore, the effects of the coupling, stacking sequence and position of the interface on the stresses, electric potential and magnetic potential were investigated.

As a result, the following results are obtained:

For the heat condition $H_a = H_b = 1.0$,

(1) The maximum of $\bar{\sigma}_{rr}$ for the stacking sequence $BaTiO_3/CoFe_2O_4$ is a compressive stress, while that for the stacking sequence $CoFe_2O_4/BaTiO_3$ is a tensile stress.

(2) The maximum tensile stress of $\bar{\sigma}_{\theta\theta}$ occurs in the magnetostrictive layer in the steady state without distinction of the stacking sequence.

(3) The maximum absolute value of the electric potential for the stacking sequence $BaTiO_3/CoFe_2O_4$ is smaller than that for the stacking sequence $CoFe_2O_4/BaTiO_3$.

(4) The maximum absolute value of the magnetic potential for the stacking sequence $CoFe_2O_4/BaTiO_3$ is larger than that for the stacking sequence $BaTiO_3/CoFe_2O_4$.

(5) The absolute values of electric potential increase and those of magnetic potential decrease with an increase in the thickness of piezoelectric layer.

(6) The coupling effect increases the thermal stress $\bar{\sigma}_{\theta\theta}$.

For the heat condition $H_a = 1.0$, $H_b = 100.0$,

(7) The maximum tensile stress of $\bar{\sigma}_{\theta\theta}$ occurs in the first layer in the transient state without distinction of the stacking sequence.

Though numerical calculation was carried out for a two-layered hollow cylinder, numerical calculation for the multilayered hollow cylinder with an arbitrary number of layer can be carried out.

References

(1) Harrshe, G., Dougherty, J.P. and Newnhan, R.E., Theoretical Modeling of Multilayer Magnetoelectric Composite, *Int. J. Appl. Electromagn. Mater.*, vol. 4 (1993), pp. 145-159.

(2) Nan, C.W., Magnetoelectric Effect in Composites of Piezoelectric and Piezomagnetic Phases, *Phys. Rev. B*., vol. 50 (1994), pp. 6082-6088.

(3) Benveniste, Y., Magnetoelectric Effect in Fibrous Composites with Piezoelecric and Piezomagnetic Phases, *Phys. Rev. B*., vol. 51 (1995), pp. 16424-16427.

(4) Nan, C.W., Bichurin, M.I., Dong, S., Viehland, D., and Srinivasan, G., Multiferroic Magnetoelectric Composites: Historical Perspective, Status, and Future Directions, *J. Appl. Phys*., vol. 103 (2008), 031101.

(5) Pan, E., Exact Solution for Simply Supported and Multilayered Magneto-electro-elastic Plates, Trans. ASME J. Appl. Mech., vol. 68 (2001), pp. 608-618.

(6) Pan, E., and Heyliger, P.R., Exact Solutions for Magneto-electro-elastic Laminates in Cylindrical Bending, *Int. J. Solids Struct.*, vol. 40 (2003), pp. 6859-6876.

(7) Babaei, M.H., and Chen, Z.T., Exact Solutions for Radially Polarized and Magnetized Magnetoelectroelastic Rotating Cylinders, *Smart. Mater. Struct*., vol. 17 (2008), 025035.

(8) Ying, J., and Wang, H.M., Magnetoelectroelastic Fields in Rotating Multiferroic Composite Cylindrical Structures, *J. Zhejiang Univ. Sci. A*, vol. 10 (2009), pp. 319-326.

(9) Wang, R., Han, Q., and Pan, E., An Analytical Solution for a Multilayered Magneto-electro-elastic Circular Plate under Simply Supported Lateral Boundary Conditions, *Smart. Mater. Struct*., vol. 19 (2010), 065025.

(10) Wang, H.M., and Ding, H.J., Transient Responses of a Magneto-electro-elastic Hollow Sphere for Fully Coupled Spherically Symmetric Problem, *Eur. J. Mech. A/Solids*, vol. 25 (2006), pp. 965-980.

(11) Wang, H.M., and Ding, H.J., Radial Vibration of Piezoelectric/Magnetostrictive Composite Hollow Sphere, *J. Sound Vib.*, vol. 307 (2007), pp. 330-348.

(12) Anandkumar, R., Annigeri, R., Ganesan, N., and Swarnamani, S., Free Vibration Behavior of Multiphase and Layered Magneto-electro-elastic Beam, *J. Sound Vib.*, vol. 299 (2007), pp. 44-63.

(13) Sunar, M., Al-Garni, A.Z., Ali, M.H., Kahraman, R., Finite Element Modeling of Thermopiezomagnetic Smart Structures, *AIAA J*., vol. 40 (2001), pp. 1846-1851.

(14) Kumaravel, A., Ganesan, N., and Sethurraman, R., Steady-state Analysis of a Three-layered Electro-magneto-elastic Strip in a Thermal Environment, *Smart. Mater. Struct*., vol. 16 (2007), pp. 282-295.

(15) Hou, P.F., Yi, T., and Wang, L., 2D General Solution and Fundamental Solution for Orthotropic Electro-magneto-elastic Materials, *J. Thermal Stresses*, vol. 31 (2008), pp.

807-822.

(16) Hou, P.F., Leung, A.Y., and Ding, H.J., A Point Heat Source on the Surface of a Semi-infinite Transversely Isotropic Electro-magneto-thermo-elastic Material, *Int. J. Eng. Sci.*, vol. 46 (2008), pp. 273-285.

(17) Xiong, S.M., and Ni, G.Z., 2D Green's Functions for Semi-infinite Transversely Isotropic Electro-magneto-thermo-elastic Composite, *J. Magnetism Magnetic Mater.*, vol. 321 (2009), pp. 1867-1874.

(18) Gao, C.F., Kessler, H., and Balke, H., Fracture Analysis of Electromagnetic Thermoelastic Solids, *Eur. J. Mech. A/Solids*, vol. 22 (2003), pp. 433-442.

(19) Wang, B.L., and Niraula, O.P., Transient Thermal Fracture Analysis of Transversely Isotropic Magneto-electro-elastic Materials, *J. Thermal Stresses*, vol. 30 (2007), pp. 297-317.

(20) Ootao, Y., and Tanigawa, Y., Transient Analysis of Multilayered Magneto-electro-thermoelastic Strip Due to Nonuniform Heat Supply, *Comp. Struct.*, vol. 68 (2005), pp. 471-480.

(21) Tanigawa, Y., Fukuda, T., Ootao, Y., and Tanimura, S., Transient Thermal Stress Analysis of a Multilayered Composite Laminated Cylinder with a Uniformly Distributed Heat Supply and [Its Analytical Development to Nonhomogeneous Materials], *JSME*, *Series* A, vol.55 (1989), pp.1133-1138.

(22) Ootao, Y., Fukuda, T., and Tanigawa, Y., Transient Thermal Stress Analysis of a Multi-Layered Composite Hollow Cylinder due to Asymmetric Heating and Its Application to Nonhomogeneous Materials, *Theoretical and Appl. Mech.,* vol.38 (1989), pp. 177-188.

(23) Ootao, Y., Tanigawa, Y., and Fukuda, T., Axisymmetric Transient Thermal Stress Analysis of a Multilayered Composite Hollow Cylinder, *J. Thermal Stresses*, vol.14 (1991), pp.201-213.

(24) Ootao, Y., Tanigawa, Y. and Nakanishi, N., Transient Thermal Stress Analysis of a Nonhomogeneous Hollow Sphere due to Axisymmetric Heat Supply, *JSME*, *Series* A, vol.57 (1991), pp.1581-1587.